Electronic Supplementary Material (ESI) for Soft Matter.

Supplementary Information

Low levels of lipid oxidation radically increase the passive permeability of lipid bilayers

Kristina A. Runas and Noah Malmstadt*

Mork Family Department of Chemical Engineering and Materials Science

University of Southern California

Los Angeles, CA

* malmstad@usc.edu

Reaction of Short Chain Poly(ethylene glycol) with Fluorescent Species

To form the small molecule used for permeation studies, amine-terminated short chain poly(ethylene glycol) was reacted with the NHS-ester of the dye NBD. A reaction scheme is shown in Figure S1. A 1:1 molar ratio of the two molecules was reacted in a 10:1 solution of chloroform:triethylamine. The reaction was held at 45°C for two hours, then 22°C for an additional eight hours. After the reaction was complete, the solution was evaporated under an argon stream. The reaction product was dissolved in MilliQ water (Millipore) before high performance liquid chromatography was used to separate the reagents from the reaction product.

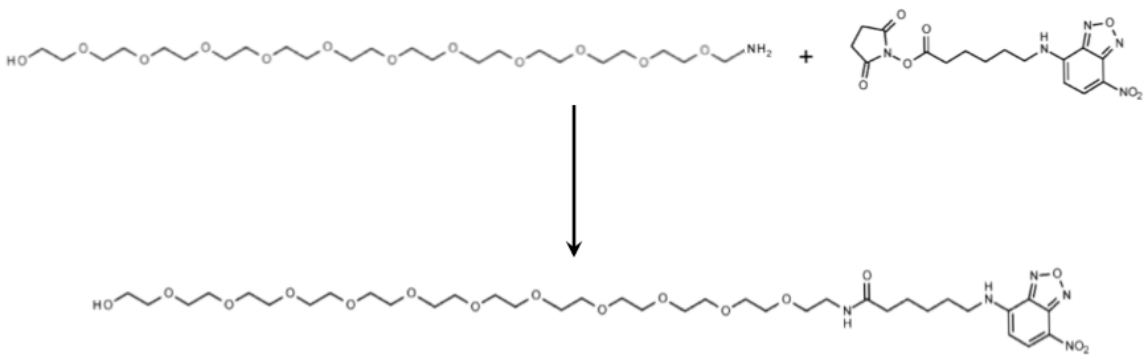

Figure S1: Reaction scheme for the preparation of the PEG12-NBD test molecule. The amine-group of the poly(ethylene oxide) alcohol reacted with the NHS-ester of the fluorescent NBD to form the fluorescent PEG species, PEG12-NBD.

The product, PEG12-NBD, was confirmed using nuclear magnetic resonance (NMR) spectroscopy. Following the reaction, peaks corresponding to the amide bond were apparent at 6.5 and 6.9 ppm.

Pinhole Crosstalk Contribution with Concentration Variation

Pinhole crosstalk is a characteristic of spinning disk confocal microscopy (SDCM) that limits the ability of the spinning disk apparatus to exclude light from regions of the sample outside of the focal plane. Previous work has been performed to establish the contribution of out-of-plane fluorescent sources to the apparent in-plane fluorescence.[1] The results showed that the pinhole crosstalk contribution from a non-focal plane scales with the square of the inverse of the distance between the non-focal and the focal plane.

During a permeability experiment with a fluorescent molecule, such as PEG12-NBD, the fluorescence inside the vesicle changes with concentration. This means that we have two sources for pinhole crosstalk: (1) fluorophore exterior to the vesicle, and (2) fluorophore inside the GUV. If the exterior fluorophore concentration is assumed to be constant, then the out of plane contribution for areas outside of the vesicle can also be assumed to be constant. However, there remains a significant out-of-plane contribution from the fluorophores inside the vesicle. This means that we need to develop a relationship between out-of-plane light contributions and fluorophore concentration inside the vesicle.

To evaluate the out-of-plane contribution for a given concentration of fluorophore inside the vesicle, GUVs were created with encapsulated 40 kDa fluorescein-dextran in 200 mM sucrose buffer at pH 7.0. 40 kDa fluorescein-dextran was chosen as it will not cross the membrane. Encapsulation concentrations were chosen between 0.1 μM and 0.5 μM to show intensities in the same range as the permeability experiments. GUVs were created with a 1:1:1 DPPC:PLinPC:Chol molar ratio, with 0.01 mol% rhodamine-DPPE.

After electroformation, GUVs were transferred to a Sykes-Moore chamber containing 200 mM glucose buffer at pH 7.0. Buffer exchange was performed until the background surrounding the vesicles showed no fluorescence intensity due to excess fluorescein-dextran. With no exterior fluorescent signal, we were able to isolate pinhole crosstalk contributions from inside the vesicle. Between 75 and 100 GUVs up to 100 um in diameter were chosen, such that for a given encapsulation concentration, the relationship between vesicle intensity and diameter could be determined.

Prior to analysis, each image was flat-fielded. As the laser alignment in a confocal microscope causes the center of the image to be brighter than the edges of the image, flat fielding will remove the dependence of GUV location on its intensity. To obtain reference images, a Sykes-Moore chamber was filled with 200 mM glucose buffer containing the concentration of 40 kDa fluorescein-dextran. Five background images were collected. For this series of background images, the value of each pixel was averaged to decrease the effect of noise. A factor was calculated that, when multiplied, made each pixel in the averaged background image equal to the mean value across the entire image. For each GUV containing the reference fluorescein-dextran concentration, the image was multiplied by this matrix of factors to generate a flat-fielded image.

After flat-fielding, the intensity and diameter of each GUV was measured using the image processing toolbox in MATLAB (MathWorks). For each concentration of encapsulated fluorescein-dextran, the relationship between vesicle intensity and diameter appears to be linear, as shown in Figure S2.

a)

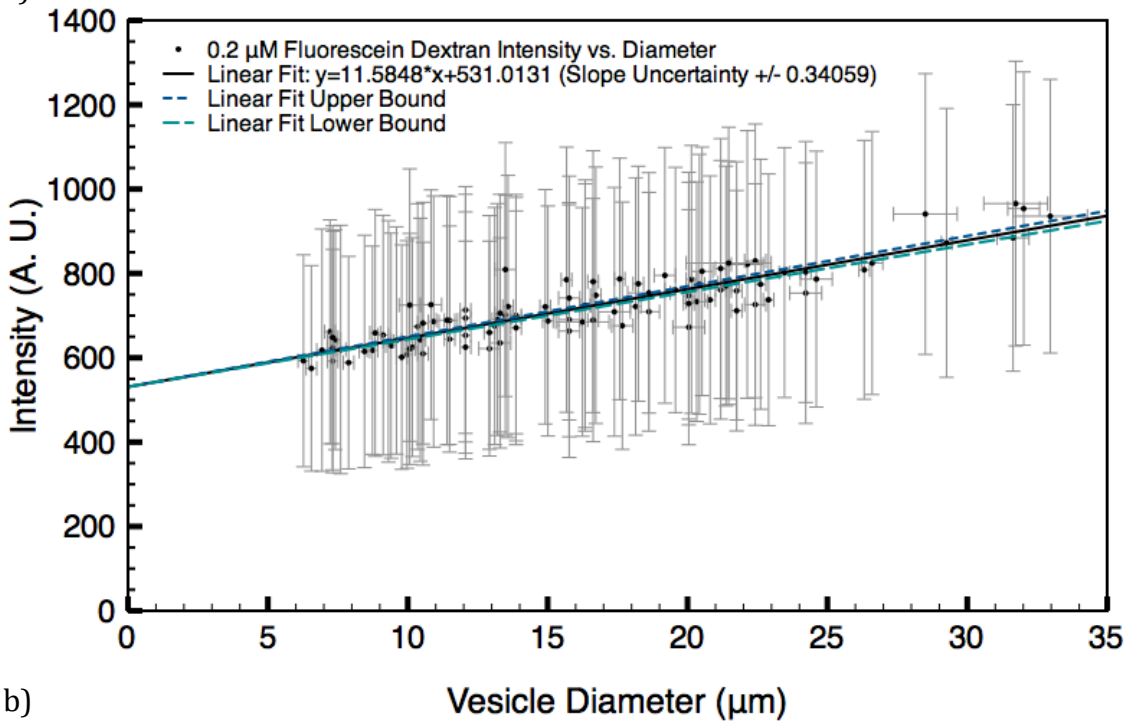

b)

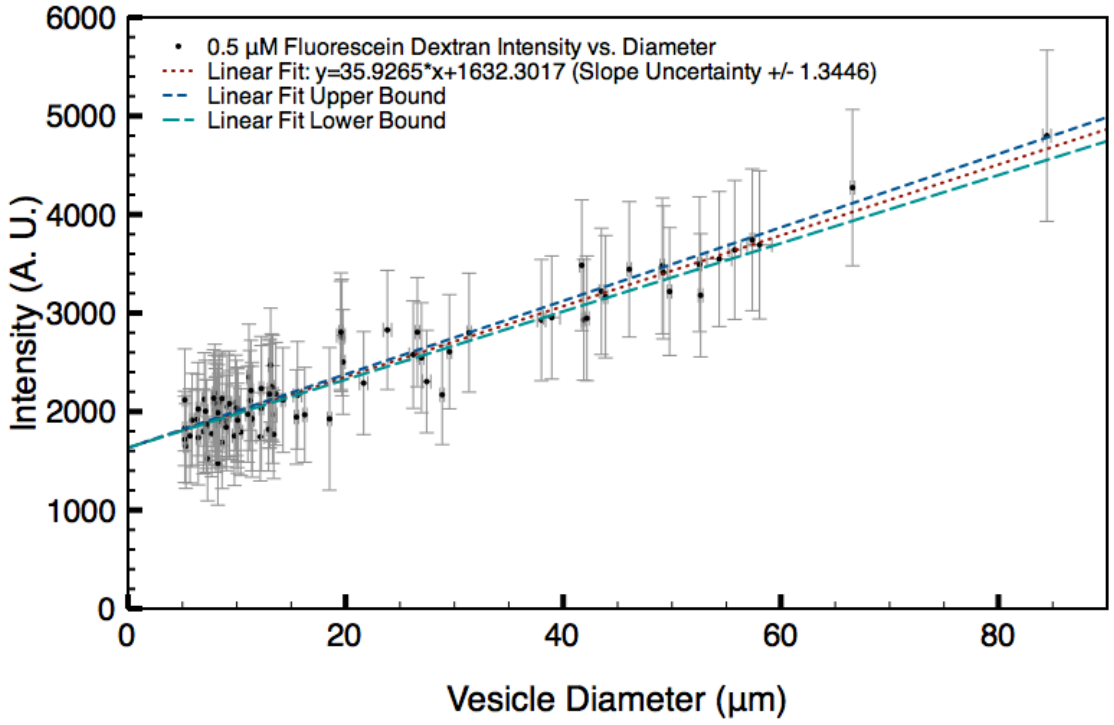

Figure S2: Linear relationship between vesicle interior intensity and diameter for a) 0.2 µM and b) 0.5 µM encapsulated 2000 kDa fluorescein-dextran. Vesicle composition was 1:1:1 DPPC:PLinPC:Chol + 0.01 mol% rhodamine-DPPE.

Assuming the y-intercept of the line is the "true" intensity of the fluorescein-dextran, then it is simple to show that for a given diameter, the pinhole crosstalk contribution is given by the difference between the actual intensity and the "true" intensity, as shown in Figure S3.

Thus, the amount of out of plane light has a dependence on both vesicle diameter and concentration. Experiments were repeated for concentrations of 0.1, 0.2, 0.3, 0.4, and 0.5 μM fluorescein-dextran, and a similar analysis was performed. The resulting linear relationships are shown in Figure S4.

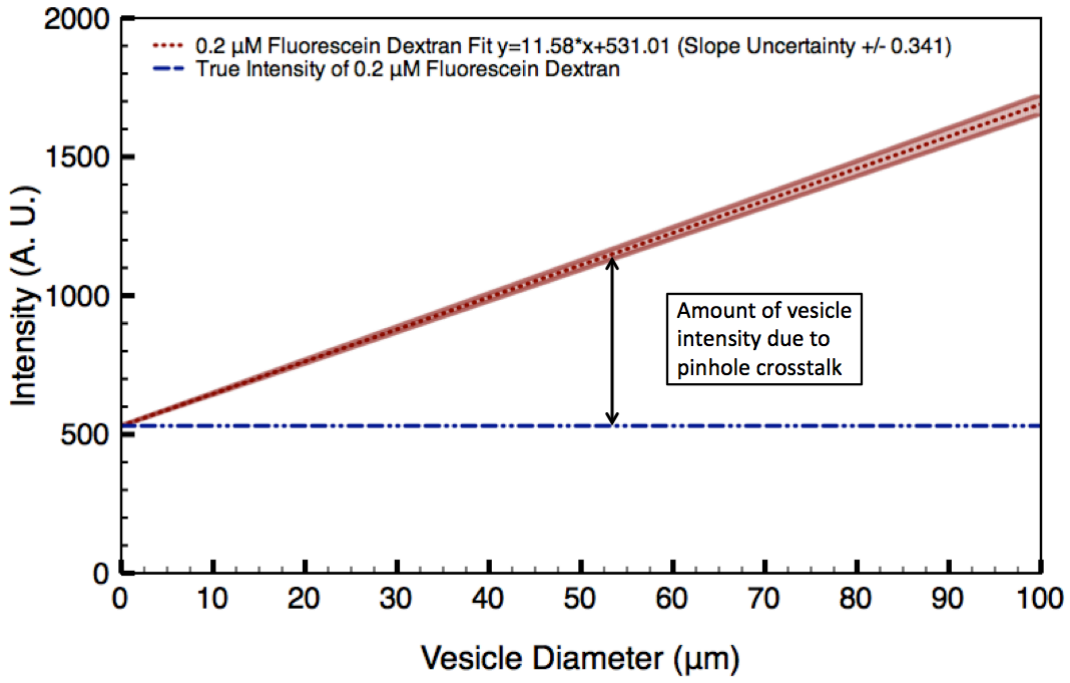

Figure S3: Vesicle interior intensity and the "true" intensity of 0.2 μM 2000 kDa fluorescein-dextran vs. vesicle diameter.

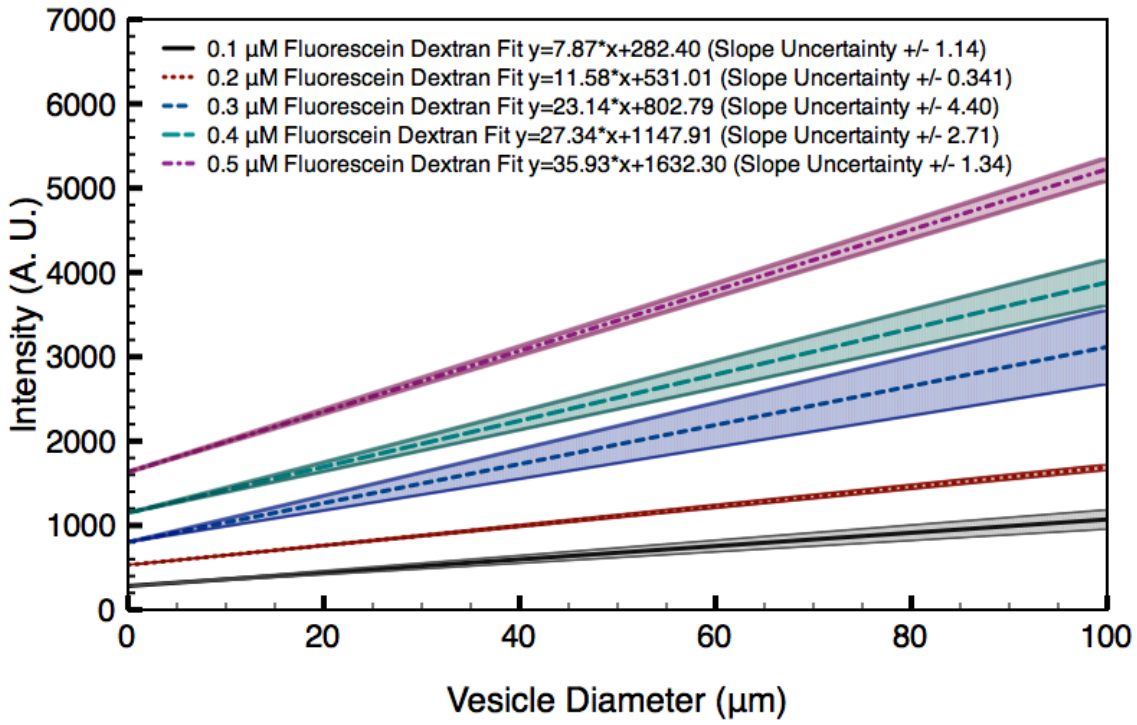

Figure S4: Linear relationships for five concentrations of encapsulated 2000 kDa fluorescein-dextran

Next, the change in out of plane with respect to concentration was evaluated for a given diameter of 1 µm. As shown in Figure S5, the relationship between the out of plane contribution and encapsulated concentration appears to be linear.

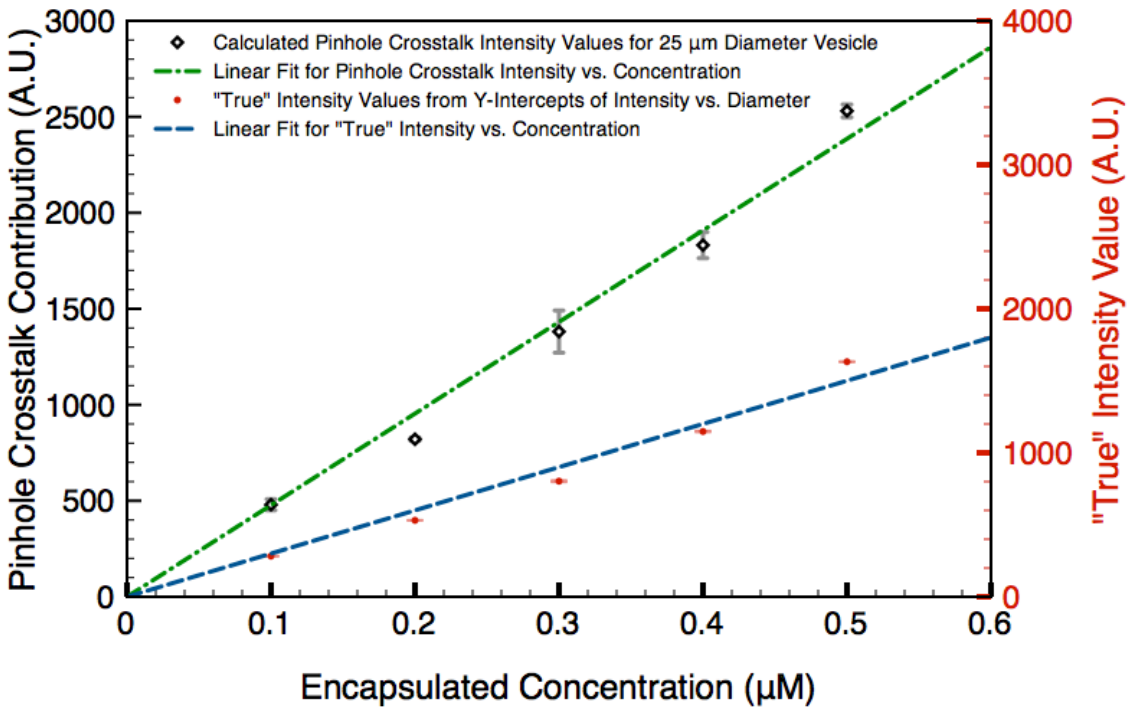

Figure S5: Linear fit for pinhole crosstalk contribution vs. concentration for 1 µm vesicle diameter

The analysis was repeated for diameters between 10 µm and 50 µm, the typical range for vesicles used in permeability experiments. For each diameter, the relationship between out of plane light and concentration is linear. The results for this diameter range are shown in Figure S6.

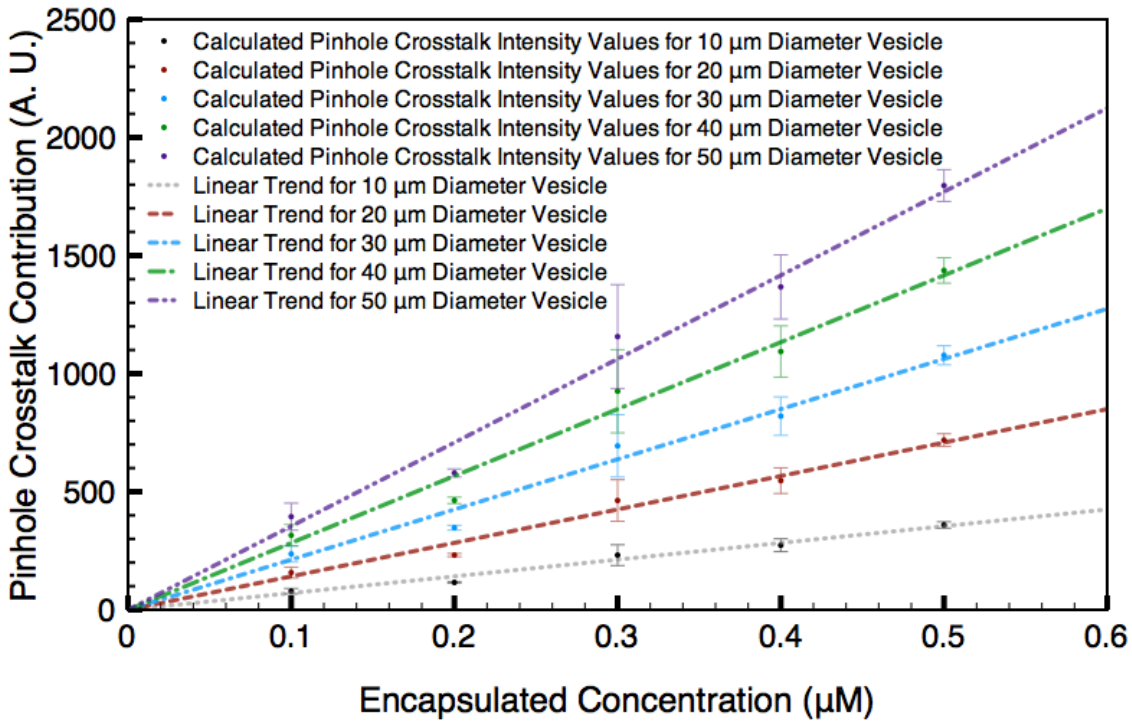

Figure S6: Linear relationships for pinhole crosstalk contribution vs. concentration for diameters between 10 and 50 µm.

From this analysis, it is clear that the out of plane light correction for fluorophore inside the GUV is dependent on both the diameter of the vesicle and the concentration encapsulated. However, for a constant diameter, the relationship with respect to concentration is consistently linear. When analyzing the permeability data, the diameter of the GUV is constant. This means that to correct for out of plane light as the concentration inside the vesicle changes, the correction should be linear with respect to concentration. We corrected for pinhole crosstalk by subtracting the crosstalk contribution predicted by the relationships shown in Figure S6 for the interior fluorophore. For the data presented, this correction factor was at most ~40% of the total intensity measured.

Pinhole Crosstalk Contribution from External Fluorophores

As mentioned above, there are two contributions to the pinhole crosstalk for a measured intensity inside of a vesicle: (1) crosstalk due to fluorophore external to the GUV, and (2) crosstalk due to fluorophore contained inside the GUV. In many cases, the external concentration can be considered to be constant over the course of an experiment, so the contribution from external fluorophores represents a constant displacement in the intensity data with no effect on the measured rate of transport or permeability. For cases where the assumption of constant external concentration breaks down (i.e. fast transport processes, compare Fig. 3b.), the change in external concentration can be neglected in analyzing the internal concentration. This is because contribution from crosstalk goes as one over the square of the distance from the focal plane.[1] Internal crosstalk is therefore much more significant than external crosstalk.

We will justify our neglecting of external crosstalk by analyzing a "worst-case-scenario" of fast transport and a small vesicle. For fast transport processes, we typically see external concentration change from 75% of the maximum to the maximum over the course of an experiment. We have previously characterized the crosstalk contribution from external fluorophores to fluorescence observed in the equatorial plane of GUVs. Based on the relationship developed by Li et al. in 2010,[2] for a 10 μm-diameter vesicle, the external crosstalk contribution represents approximately 25% of the intensity observed in the equatorial plane. Since in our experiments, there is a ~25% change in this 25% contribution, the total observed change in intensity due to non-constant external

concentration is about 6%; much less than the ~40% contribution from internal crosstalk and within imaging error.

Finite Difference Model

The finite difference approach was adapted from Somersalo et al.[3] The advantage of their technique was in the decoupling of the time and space dimensions, and solving the system as a matrix equation. This allowed for fast convergence of the model. An example result from the finite difference model is shown in Figure S7. The model takes the background intensity as the concentration boundary condition at the vesicle exterior. At each time point, the model then calculates the concentration along a series of space steps. For the space step representing the membrane, a flux boundary condition incorporates the membrane permeability into the model. The concentration is then calculated for the space steps contained inside the vesicle membrane; at the vesicle center, a no-flux boundary condition is applied. This process is repeated for each time step until equilibrium is reached or the data set is complete. For Figure S7, the center of the vesicle is located at 0 μm along the x-axis. The radius of the vesicle is 25 μm, so the membrane is located at this point on the x-axis. The step size in the x-dimension was 0.5 μm. Diffusivity of the PEG12-NBD molecule in water is 3.6×10^{-6} cm^2/s.[4] The y-axis represents the intensity at each special location, and the color gradient shows the time series. The permeability of the membrane, as calculated by the model, was 2.86×10^{-6} cm/s.

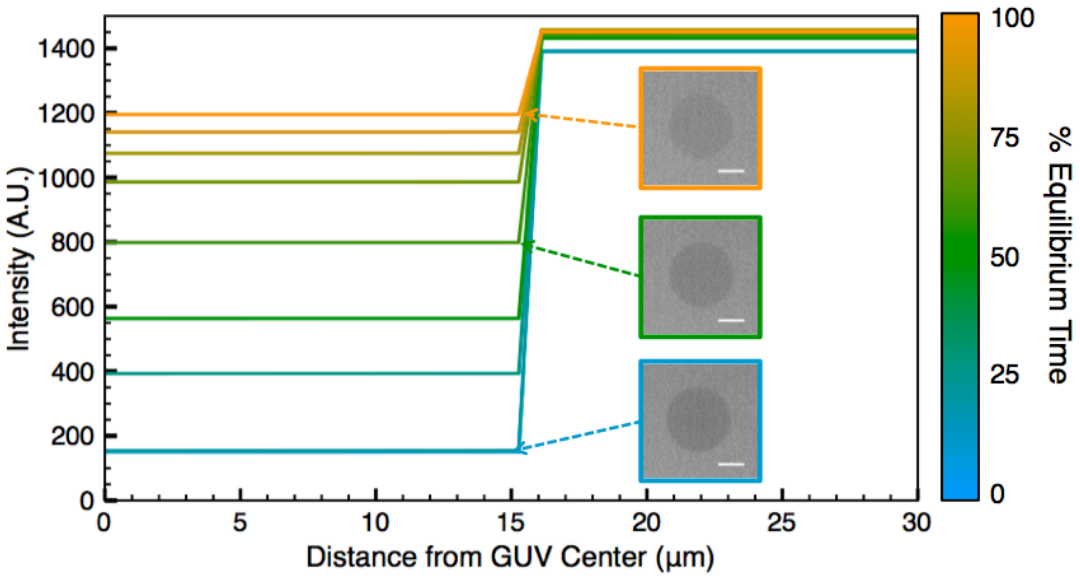

Figure S7: Results from a finite difference simulation of 0% POxnoPC. Diffusivity of the permeating species, PEG12-NBD, was 3.6×10^{-6} cm^2/s.[4] The vesicle center is located at 0 along the x-axis, with the membrane location at 15 µm. Step size in the x-dimension was 0.5 µm. The y-axis indicates the percentage of the background concentration, and the color gradient indicates different time points during the permeation process. In this manner, the model can show both spatial and time variation of concentration. The insets show images from the transport experiment corresponding to certain time points. The permeability indicated by the model was 2.8×10^{-6} cm/s. Scale bar is 10 µm.

To use this model to calculate the membrane permeability, the finite difference model is used to solve the system for various values of permeability at the membrane boundary. The observed experimental intensity at the vesicle center is compared to the modeled intensity at the vesicle center. The resulting concentration vs. time curve for the data set and the best fit model results is shown in Figure S8.

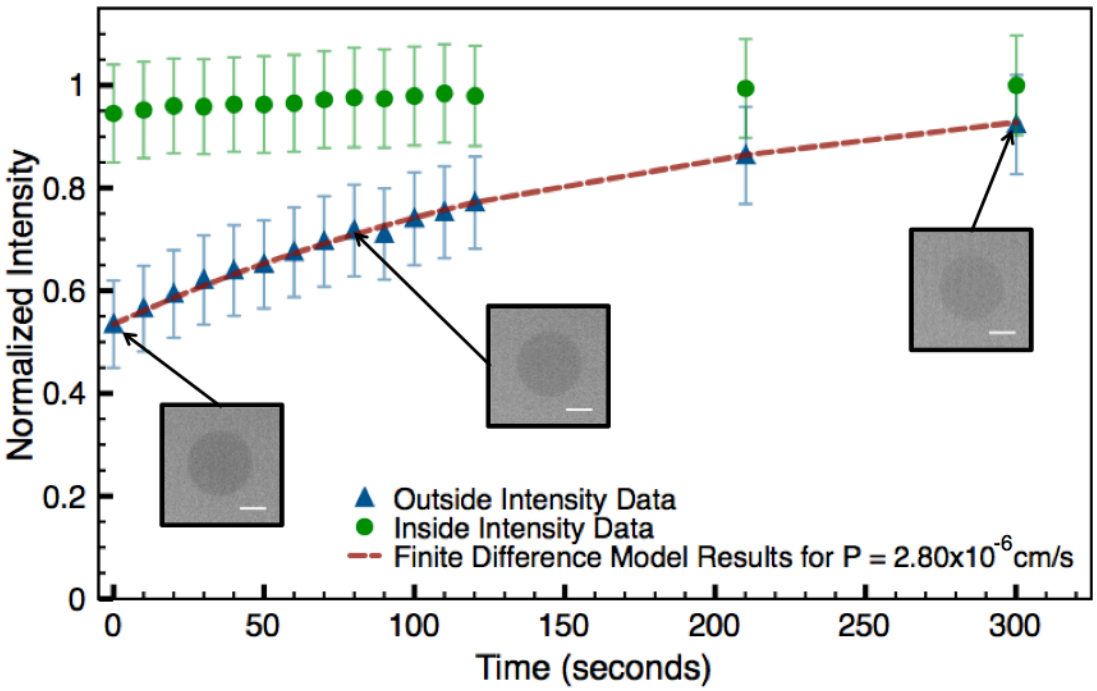

Figure S8: Intensity data and resulting fit for a data set with 0% POxnoPC. This data corresponds to the finite difference model shown in Figure S7. The green data points indicate the normalized intensity data at the vesicle exterior, the blue indicate normalized intensity data at the vesicle center. The red line indicates the results of the finite difference model for the best fit permeability. Image scale bars are 10 μm. The permeability of the 0% POxnoPC data shows a permeability of 2.80×10^{-6} cm/s.

To determine the best fit, the χ^2 value for model vs. experimental intensity curves was calculated at a range of model permeabilities. χ^2 is minimized using the 'fminsearch' routine in Matlab. The χ^2 landscape with respect to permeability was used to determine the uncertainties of the model result, with a p-value of 0.05. An example chi-squared landscape is shown in Figure S9. These results correspond to the data set shown in Figures S7 and S8.

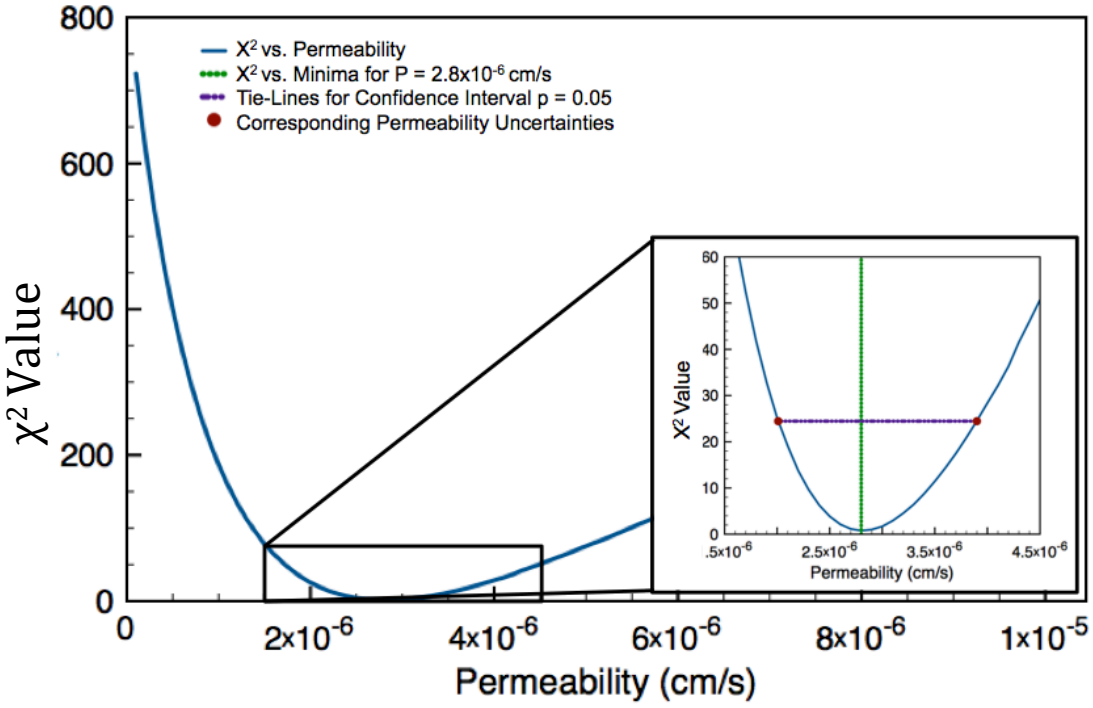

Figure S9: χ^2 landscape for a data set of 0% POxnoPC. The minimum χ^2 value corresponds to the permeability from the best fit of the model. The inset panel shows a close up view of the minimum χ^2 value. A chosen critical value of p = 0.05 corresponds to a χ^2 greater than this minimum; at this χ^2, the uncertainty of the permeability can be calculated. The critical value indicates the +/- of the permeability for that degree of certainty (shown in purple on the inset).

Permeability and Vesicle Diameter

The addition of the POxnoPC caused an overall decrease in vesicle size. Figure S10 shows the average diameter measured for each of the compositions analyzed in the main text. From the analyzed data points, the diameter is shown to decrease with increased amounts of oxidation. This decrease in vesicle size is not unexpected: previous research has demonstrated the changes in membrane curvature and budding due to lipid oxidation.[5] The cleaved tail group has been associated with decreased lipid area and corresponding decreases in membrane area.[6]

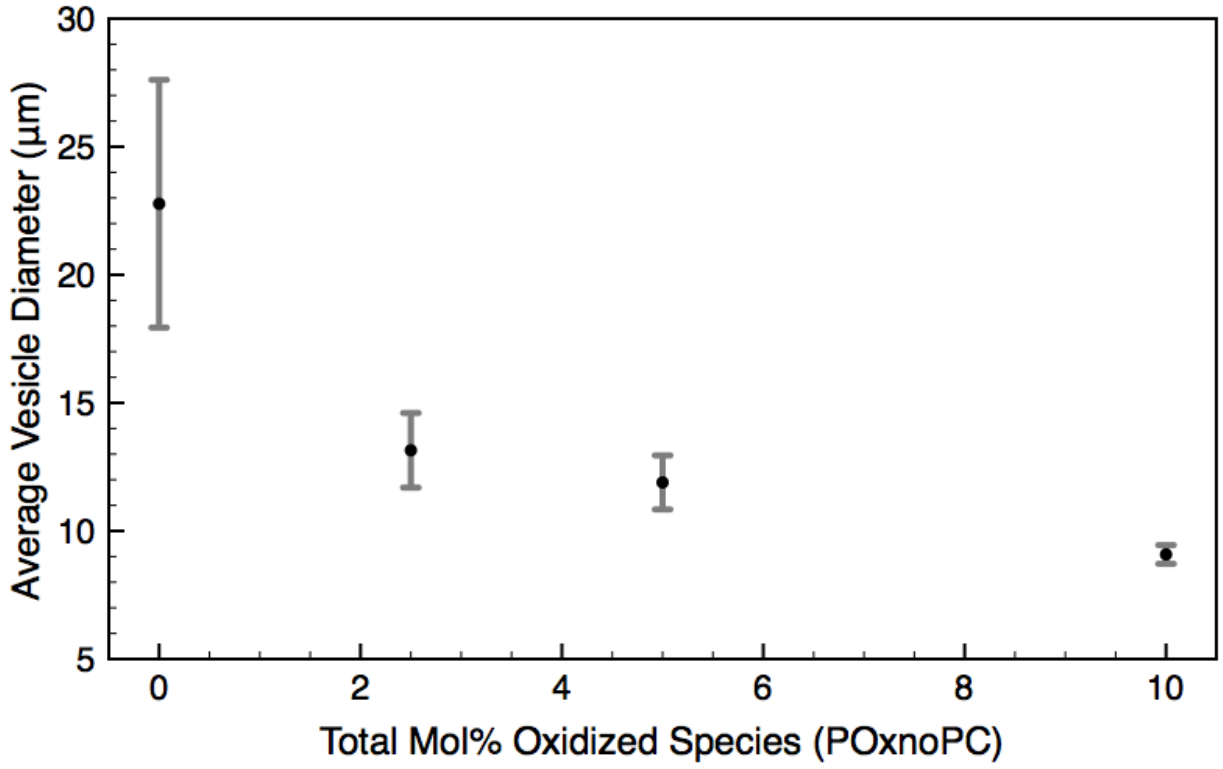

Figure S10: Correlation between vesicle diameter and percent oxidation. The average vesicle diameter was calculated for each of the four compositions measured for permeability (shown in Figure 4 of the main text). As oxidation increases, overall vesicle size decreases. Despite this trend, there does not appear to be a correlation between measured permeability and vesicle diameter, as shown in Figure S11.

It is important to note, however, that the permeability does not appear to be correlated with the diameter. Figure S11 plots permeability for all vesicles observed as a function of vesicle diameter. While the trend shown in Figure S10 clearly results in clustering—0% POxnoPC vesicles are big and relatively impermeable in comparison to other compositions—there is no discernable dependence of permeability of vesicle size within the two clusters.

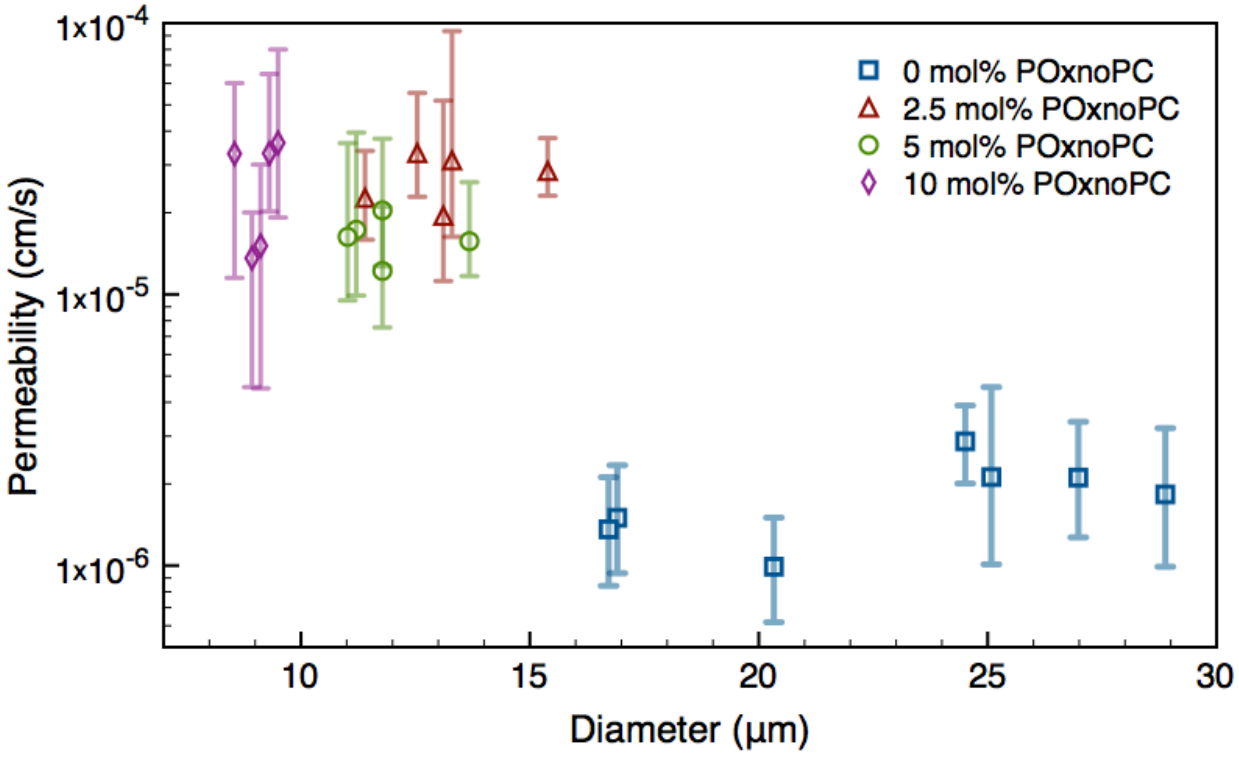

Figure S11: Measured permeability vs. vesicle diameter for four levels of lipid oxidation. There does not appear to be a correlation between measured permeability and vesicle diameter. The permeability was plotted vs. diameter for vesicles containing various amounts POxnoPC. There does not appear to be a trend between these two parameters.

Biotin-DPPE and Measured Permeability

Since biotin-DPPE was used to immobilize the vesicles to the surface of the microfluidic channel, we examined the effect of biotin-DPPE concentration on the measured permeability. To test if the presence of biotin-DPPE had an effect on membrane permeability, we varied the amount of biotin-DPPE present in the membrane then measured the permeability. We chose two levels of oxidation (0 mol% POxnoPC and 10 mol% POxnoPC) to examine. For each of these oxidation points, we decreased the biotin-DPPE concentration from 6 mol% to either 4 mol% or 2 mol%. Results for these tests are

shown in Figure S12. There is no apparent effect of biotin-DPPE on the membrane permeability.

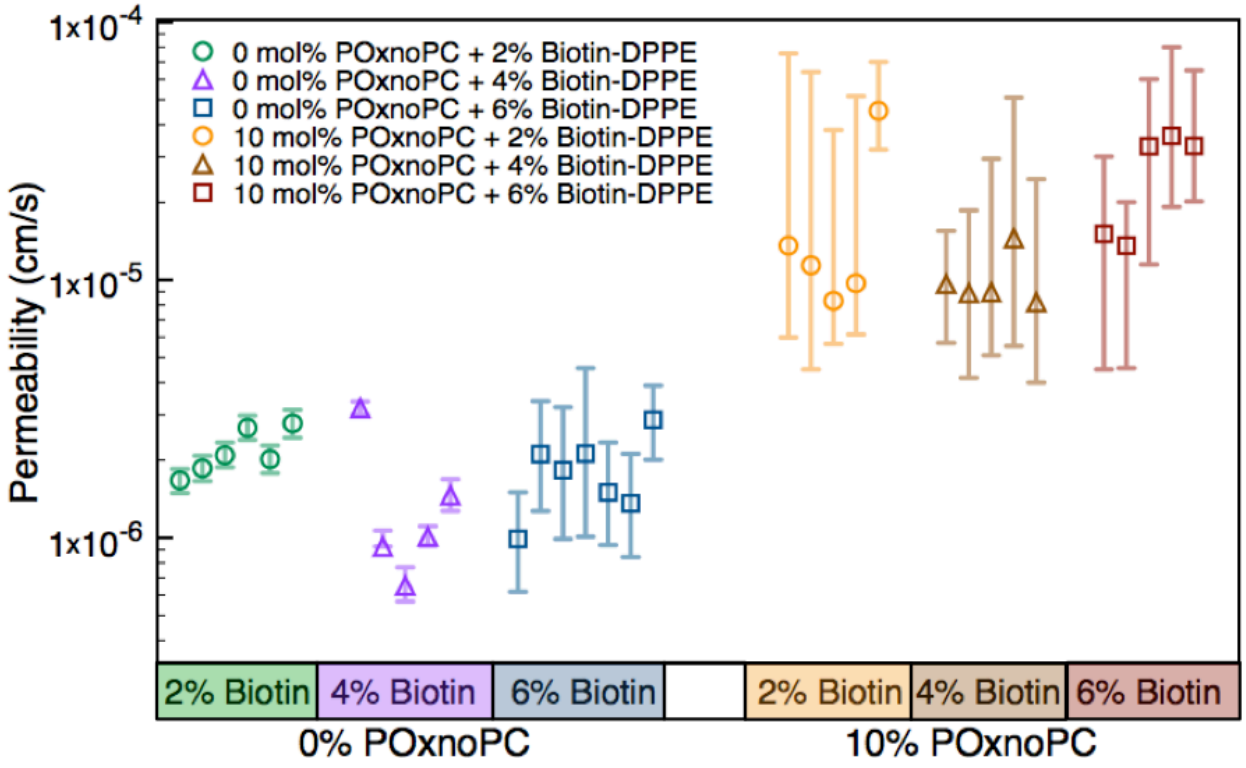

Figure S12: Measured permeability vs. mol % biotin-DPPE for two levels of oxidation: 0 mol% and 10 mol% POxnoPC. For each composition, permeability does not appear to depend on biotin-DPPE concentration.

REFERENCES

(1) Sandison, D. R., Webb, W. W. Background Rejection and Signal-to-Noise Optimization in Confocal and Alternative Fluorescence Microscopes. *Appl. Opt.* **1994,** *33*, 603-615.

(2) Li, S., Hu, P. C., Malmstadt, N. Imaging Molecular Transport across Lipid Bilayers. *Biophys. J.* **2011,** *101*, 700-708.

(3) Somersalo, E., Occhipinti, R., Boron, W. F., Calvetti, D. A Reaction–Diffusion Model of Co 2 Influx into an Oocyte. *J. Theor. Biol.* **2012,** *309*, 185-203.

(4) Li, S., Hu, P., Malmstadt, N. Confocal Imaging to Quantify Passive Transport across Biomimetic Lipid Membranes. *Anal. Chem.* **2010,** *82*, 7766-7771.

(5) Heuvingh, J., Bonneau, S. Asymmetric Oxidation of Giant Vesicles Triggers Curvature-Associated Shape Transition and Permeabilization. *Biophys. J.* **2009,** *97*, 2904-2912.

(6) Sankhagowit, S., Biswas, R., Wu, S.-H., Riche, C. T., Povinelli, M. L., Malmstadt, N. The Dynamics of Giant Unilamellar Vesicle Oxidation Probed by Morphological Transitions. *Biochimica et Biophysica Acta***,** *1828*, 2615-2624.